View metadata, citation and similar papers at core.ac.uk
brought to you by CORE
provided by Università degli Studi di Napoli Federico II Open Archive

UNIVERSITA' DEGLI STUDI DI NAPOLI "FEDERICO II"

FACOLTA' DI FARMACIA
DIPARTIMENTO DI CHIMICA FARMACEUTICA E TOSSICOLOGICA

Dottorato di Ricerca in
Scienza del Farmaco XXIII ciclo

Identification of Novel Molecular Scaffolds for the Design of MMP-13 Inhibitors through Virtual Screening Methods

Coordinatore
Chiar.ma Prof.ssa
MARIA VALERIA D'AURIA

Supervisore
Chiar.ma Prof.ssa
LUCIANA MARINELLI

Candidato
VALERIA LA PIETRA

“I stand at the seashore, alone, and start to think. There are the rushing waves ... mountains of molecules, each stupidly minding its own business ... trillions apart ... yet forming white surf in unison.

Ages on ages ... before any eyes could see ... year after year ... thunderously pounding the shore as now. For whom, for what? ... on a dead planet, with no life to entertain.

Never at rest ... tortured by energy ... wasted prodigiously by the sun ... poured into space. A mite makes the sea roar.

Deep in the sea, all molecules repeat the patterns of one another till complex new ones are formed. They make others like themselves ... and a new dance starts.

Growing in size and complexity ... living things, masses of atoms, DNA, protein ... dancing a pattern ever more intricate.

Out of the cradle onto the dry land ... here it is standing ... atoms with consciousness ... matter with curiosity.

Stands at the sea ... wonders at wondering ... I ... a universe of atoms ... an atom in the universe. ”

"The Value of Science"

Richard P. Feynman

Acknowledgements

I would like to thank all people who have helped and inspired me during my doctoral study.

I am indeed very grateful for the guidance of Prof. Novellino that was bountifully helpful and offered invaluable assistance and support. I also would like to thank my supervisor, Prof.ssa MariaValeria D'Auria, for all her advice and encouragement.

I especially want to show gratitude to my advisor, Prof. Luciana Marinelli, for her mentoring during my research and study. Her perpetual energy and enthusiasm in research and life had motivated and inspired me through all these years. I cannot quantify the impact of Luciana on this project, she kept me focused and yet provided me with a lot of independence, she was a guide, a master, an example, a friend, sometimes a sister, it is clear that without her the outcomes of my research and the direction of my life would have been different.

My year stint at Yale University opened my mind and motivated me. I thank Prof. William Jorgensen for allowing me to join his group; it was an honor for me to work in his laboratory, his experience and his kindness will always be greatly treasured.

At times, a PhD can be quite stressful and I feel fortunate to have completed it in a friendly environment. All my lab buddies had stimulated me in research and life through our interactions during the long hours in the lab. Thanks to all of them and especially to Dr. Sandro Cosconati.

My deepest gratitude goes to my family for their unflagging love and support throughout my life; this dissertation is simply impossible without them. I am thankful to my father, for his care and love. I cannot ask for more from my mother, as she is simply perfect. I have no suitable words that can fully describe their everlasting love to me.

I kept the last paragraph for you Marco. Meeting you was a blessing and ever since then I feel you gave my life a higher meaning. I sense your presence behind everything I do and I cannot see purpose without you. Thank you.

Contents

Chapter I

Chapter II

Result and Discussion

Experimental Section

1. INTRODUCTION

1.1 MMP-13 and the Osteoartrite (OA) desease

Osteoarthritis (OA) is the leading cause of joint pain and disability in middle-aged and elderly patients. It is characterized by progressive loss of articular cartilage that eventually leads to denudation of the joint surface. The cartilage loss observed in OA is the result of a complex process involving degradation of various components of the cartilage matrix. Particularly, degradation of cartilage-specific type II collagen by mammalian collagenases (MMPs) is a key step in the loss of structural and functional integrity of cartilage.[1] Among all known MMPs, MMP-13 is considered the principal target in OA. Indeed, today there are overwhelming data on the role of MMP-13 in the pathogenesis of OA,[2] and inhibition of its activity has proven to be efficacious in a variety of models of experimentally induced as well as spontaneously occurring OA.[3] Unfortunately, none of the known MMP inhibitors (MMPIs) have been successfully utilized as therapeutic agents so far. This was due to the lack of selectivity for a specific isozyme, leading to heavy dose- and duration-dependent musculoskeletal side effects.[4] Therefore, current drug development strategies for treatment of OA are focused on selective inhibition of MMP-13, although recent evidences suggest that other MMPs, such as MMP-1, may also contribute to the collagen degradation process.[5] However, the design of a selective MMPI is not a trivial task, as

MMPs share an high similarity in the overall three-dimensional fold and many conserved amino acids exist in the inhibitor binding site, besides the conserved catalytic zinc ion. The major structural difference observed between the MMP enzymes resides in the relative size and shape of the S1' subsite, which is located in proximity of the catalytic metal. From a structural point of view, almost all MMPIs known so far are based on a zinc-binding group (ZBG) and a hydrophobic portion protruding into the hydrophobic S1' subsite. These compounds behave as competitive inhibitors since the ZBG can mimic one of the transition states occurring during the substrate hydrolysis. Currently, two successful strategies to confer selectivity of action to an MMP inhibitor are known: the first resides in the proper modification of the P1' substituent on MMPI to take advantage of the differences between the diverse MMPs; the second is the finding of an allosteric inhibitor,[6] which binds tightly to the S1' and S1'* subsite without chelating the metal that is thought to contribute to the promiscuous inhibition of multiple MMPs.**Errore. Il segnalibro non è definito.**c Recently, as a result of the first strategy, it has been designed a *N*-isopropoxy-arylsulfonamide-based hydroxamate inhibitor, which showed low nanomolar activity for MMP-13 and high selectivity over some other tested MMPs.[7] In parallel to further studies aiming to assess the activity of this promising compound using *in vivo* models of OA, it has been decided to seek for novel scaffolds as allosteric inhibitors on one hand, and as zinc-chelating non-hydroxamate inhibitors on the other. In fact, a debate is still

open on the advisability of using hydroxamates as ZBG due to toxicity and metabolic stability issues.[8,9]

In this respect, we have taken advantage of the availability of several MMP-13 crystal structures and have used two different in silico methods to screen the Life Chemicals and the Maybridge databases, respectively. Experimental tests of a limited selection of candidate compounds (60) verified nine novel leads, structurally unrelated to the known MMPIs.

1.2 MMPs: Definition, Function and Regulation.

Matrix metalloproteinases (MMPs) are a family of extracellular zinc-dependent neutral endopeptidases collectively capable of degrading essentially all ECM components and they play an important role in ECM remodeling in physiologic situations, such as embryonal development, tissue regeneration, and wound repair. MMPs also play a role in pathological conditions involving untimely and accelerated turnover of ECM, including rheumatoid arthritis, osteoarthritis, atherosclerotic plaque rupture, aortic aneurysms, periodontitis, autoimmune blistering disorders of the skin, dermal photoaging, and chronic ulcerations. In addition, distinct MMPs play important, and sometimes opposite roles at different steps of tumor growth, invasion, and metastasis, and recent observations suggest that MMPs also play a role in cancer cell survival.

The human MMP gene family consists of more than 25 structurally related members that fall into five classes according to their primary structure and substrate specificity: collagenases (MMP-1, MMP-8, and MMP-13), gelatinases (MMP-2 and MMP-9), stromelysins (MMP-3, MMP-7, MMP-10, MMP-11, and MMP-12), membrane type (MT)-MMPs (MT1-MMP, MT2- MMP, MT3-MMP, and MT4-MMP), and nonclassified MMPs[10]. The proteolytic activity of MMPs is inhibited by nonspecific protease inhibitors, such as α2-macroglobulin and α1- antiprotease, and by the specific tissue inhibitors of the metalloproteinases (TIMPs). The TIMPs

are a family of four structurally related proteins (TIMP-1, -2, -3, and -4), which exert a dual control on the MMPs by inhibiting both the active form of the MMPs and their activation process. The TIMPs inhibit the enzymatic activity of all members of the MMP family (with the exception of MT1-MMP, which is inhibited by TIMP-2 and -3 but not by TIMP-1) by forming noncovalent stoichiometric complexes with the active zinc-binding site of the MMPs.[11]

The general structure of the MMPs includes a signal peptide, a propeptide domain, a catalytic domain with a highly conserved zinc-binding site, and a haemopexin-like domain that is linked to the catalytic domain by a hinge region. In addition, MMP-2 and MMP-9 contain fibronectin type II inserts within the catalytic domain, and MT-MMPs contain a transmembrane domain at the C-terminal end of the haemopexin-like domain. The haemopexin domain is absent in the smallest MMP, like matrilysin (MMP-7).

Most MMPs are secreted as latent precursors (zymogens) that are proteolytically activated in the extracellular space. The pro-MMPs are retained in their inactive form by an interaction between a cysteine residue located in the propeptide portion of the molecule with the catalytic zinc atom, blocking the access of substrates to the catalytic pocket of the enzyme. Partial proteolytic cleavage of the propeptide dissociates the covalent bond between the cysteine residue and the catalytic site and exposes the catalytic site to the substrate. MMPs are activated in an orderly

fashion, with one activated MMP cleaving and activating the next in a complex and only partially deciphered network of proteases in the extracellular space.[12]

The catalytic domain is folded into a single globular unit approximately 35 Å in diameter and the structure is dominated by a single five-stranded β–sheet with one antiparallel and four parallel strands and three α-helices. The catalytic domain contains two tetrahedrally–coordinated Zn2+ ions: a “structural” zinc ion and a “catalytic” zinc ion whose ligands include the side chains of the three histidyl residues in the conserved HEXXHXXGXXH sequence.

To date, eighteen X-ray structures of MMP-13 catalytic domain have been released in the Protein Data Bank. Besides that co-crystallized with TIMP-2 (PDB code: 2E2D), all the others were co-crystallized with organic inhibitors. A superposition of all X-ray structures on the alpha carbon atoms, using 830C as reference structure, shows that the protein folding and the catalytic loops shape are highly superimposable. Intriguingly, the analysis of these complexes reveals that some inhibitors do not bind the catalytic zinc ion, but they only tightly occupy the S1’ pocket. Furthermore, these so called allosteric inhibitors possess a very peculiar shape that allow them to explore also an adjacent cavity named S1’*, which is unique among all the other MMPs. In these cases, the secondary and tertiary structures of the enzyme in general resemble those described for MMP13 crystallized with zinc binding inhibitors,[13] except in

the S1'-specificity loop.[14] It is evident that the non-zinc binding MMP13 inhibitors confer an ordered structure to the S1'-specificity loop that is otherwise flexible and poorly defined. Particularly, the most active allosteric inhibitor, a methylquinazoline-dione compound, cocrystallized in 2OZR pdb structure (Fig 1),[15] does not interact with zinc ion but instead binds deep within the S1'-specificity loop of the protein and extends past this pocket out toward solvent. The benzyl ester points toward the substrate binding cleft but overlaps only slightly with the space that would be occupied by a P1' leucine amino acid side chain in productively bound substrates or in non-selective peptidic MMP inhibitors such as GM-6001. This binding mode is consistent with a non-competitive mechanism of inhibition and contrasts with the substrate competitive inhibition expected for MMP inhibitors that bind to the catalytic zinc ion. In addition to not binding the catalytic zinc ion, this inhibitor does not occupy space within the substrate binding cleft of MMP-13. Its inhibitory potency and target specificity can be explained by complementarities of the inhibitor and the accommodating S1'-specificity loop of MMP13 in which it binds. This structural information represents the molecular underpinnings for the identification and/or the design of novel, selective and potent allosteric inhibitors.

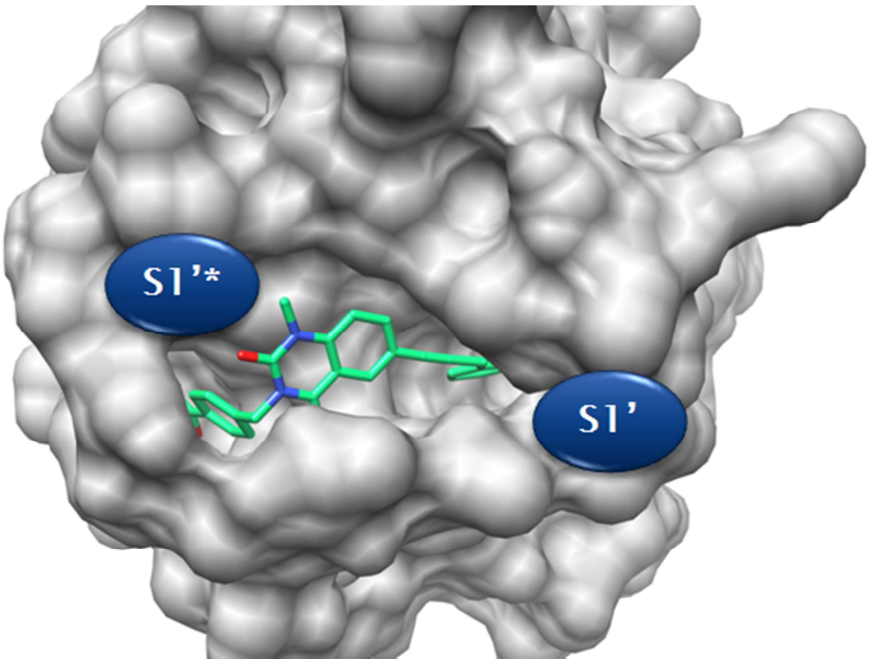

Figure 1. Crystal structure 2OZR with the most active allosteric inhibitor.

1.3 State-of-the-art Methodologies

In the early stage of research of drug discovery programs, high-throughput screening (HTS) procedures can be applied for hit identification in large small molecule databases. In the past decade, in silico screening has been extensively used to reduce the number of compounds going into HTS, reducing time and costs for hit finding. In this respect, Virtual Screening (VS) is a technique now commonly used in drug discovery programs for lead finding and optimization and for scaffold hopping.[16] In such an approach, a collection of potential candidate compounds is screened against a target protein or a reference molecule in order to select a subset of compounds for effective experimental screening. The selection can be done using a wide range of VS methods, either ligand- or target-based when the three-dimensional (3D) structure of the target protein is available.

The classical straightforward concept aiming at identifying analogues by comparing the physicochemical, structural, or pharmacophoric properties of a known active molecule with that of compounds in a collection has been massively applied during the last decades. Initially, these ligand-based virtual ligand screening (LBVLS) methods were based on simple 2D descriptors or fingerprints[17] derived from the structure of the reference active compound and compared to the corresponding descriptors of database compounds using a similarity metric, such as the Tanimoto

coefficient (Tc). These methods were generally efficient, very fast, and provided as a result hits sharing a common chemotype with the active molecule used as the reference.[18] To increase the structural diversity of the hits provided by LBVLS methods and thus to perform "scaffold-hopping" (i.e., change the chemotype, keep the activity[19]), different methods using more sophisticated 3D descriptors have later been developed, such as pharmacophore screening[20] or shape similarity searching.[21]

In pharmacophore screening, the knowledge of a set of aligned known active compounds is required, in contrast to shape similarity search methods that only require the structure of a single active compound. Shape similarity search methods thus appear as the LBVLS methods of choice when the structure of only few compounds is available.

Finally, when the structure of the target in complex with a ligand is available, structure-based virtual ligand screening (SBVLS) methods like docking/scoring[22] or structure-based pharmacophore screening[23] are generally preferred.

In this thesis work the author explores the proficiency of ROCS and Autodock 4.0 programs for the fast and effective identification of novel bioactive inhibitors of MMP-13 from two different databases.

ROCS is a fast shape comparison application, based on the idea that molecules have similar shape if their volumes overlay well and any volume mismatch is a measure of dissimilarity. It uses a smooth Gaussian function

to represent the molecular volume,[24] so it is possible to routinely minimize to the best global match.

ROCS is a powerful virtual screening tool which can rapidly identify potentially active compounds with a similar shape to a known lead compound.[25] The high speed of ROCS enables the screening of entire multi-conformer corporate collections in a single day on a single processor. Recent work indicates that ROCS is competitve with, and often superior to, structure-based approaches in virtual screening,[26,27] both in terms of overall performance and consistency.[28] ROCS alignments to crystallographic conformations have also been useful in pose prediction in the absence of a protein structure.[29]

On the other hand, AutoDock 4.0[30] has been used as a suite of automated docking tools. As one of the most widely used docking program, it is designed to predict how small molecules, such as substrates or drug candidates, bind to a receptor of known 3D structure. AutoDock actually consists of two main programs: AutoDock performs the docking of the ligand to a set of grids describing the target protein; AutoGrid pre-calculates these grids. AutoDock 4.0 is faster than earlier versions, and it allows sidechains in the macromolecule to be flexible. AutoDock 4.0 has a free-energy scoring function that is based on a linear regression analysis, the AMBER force field, and a large set of diverse protein-ligand complexes with known inhibition constants. This novel force field (FF), accounting for an improved thermodynamic model, allows to more

accurately simulate the ligand/receptor binding process in comparison to the older version.

II. Results and Discussion.

2.1 Receptor-Based Virtual Screening. AutoDock4.

To date, eighteen X-ray structures of MMP-13 have been released in the Protein Data Bank. Besides that co-crystallized with TIMP-2 (PDB code: 2E2D), all the others were co-crystallized with organic inhibitors such as the diphenylether sulfone RS-130830 (PDB code 830C). A superposition of all X-ray structures on the alpha carbon atoms, using 830C as reference structure, shows that the protein folding and the catalytic loops shape are highly superimposable, and that in the catalytic site the large majority of the residues are all preserved in the side chain conformations. Thus, only the enzyme structure 830C, which has the lower resolution (1.60 Å), was selected for our VS experiment. As docking program for the VS, we used the Autodock program (AD4), which has been extensively and successfully employed in multiple VS campaigns undertaken by our research group.[31] AD4 was applied to virtually screen the Life Chemicals database, a collection of six thousands non-redundant drug-like compounds selected to provide the broadest pharmacophore coverage. Prior to docking experiments, the entire Life Chemicals database was processed with the ZINC protocol leading to a total of 7769 molecules (see Experimental section for details). The results of the VS on the Life Chemical database, were then sorted on the basis of the predicted binding free energies (ΔG_{AD4}) which in our case ranged from -3.93 to -15.61 kcal/mol. A scoring filter was set arbitrarily to -10.5 kcal/mol so as to retain 23% of the docked

solutions. The top 1800 compounds in their predicted binding poses were selected for visual inspection. In order to obtain compounds endowed with an inhibitory potency against MMP-13, we discarded all the molecules for which AD4 did not predict coordination of the catalytic zinc. Then, in the attempt to find leads with a certain selectivity of action, for each inspected compound, the occupancy of the S1' pocket has been evaluated, although it was not expected to be total due to the small size of the docked compounds. As last criterion of choice, we evaluated the attitude of each molecule to be chemically optimized. At the end of this process, a total of 24 compounds of the Life Chemical Data Set were selected for further analysis. Two products were not available from the vendor, and two were not soluble at the test concentration, so a total of twenty compounds were used for biochemical assays. Initially, all compounds were screened at a concentration of 100 μM by fluorometric assay on recombinat enzyme. ARP100,[32] a hydroxamate-based MMP inhibitor previously developed by our research group, was used in the same assay conditions as reference compound. To exclude any possible nonspecific/promiscuous inhibition of MMP-13 due to aggregate formation, we performed all the assays pertaining the active compounds in the presence of 0.05% Brij-35, a nonionic detergent similar to Triton X-100, as suggested by Shoichet et al.[33] Five ligands, out of the twenty tested, provided considerable inhibition of MMP-13 activity and were characterized in detail (see Experimental Methods). All other compounds that did not cause detectable inhibition at

100 μM concentrations were not further investigated (see SI for chemical structures). Table 1 lists structures, Life Chemicals codes, AD4 binding free energies and the MMP-13 IC_{50} of the novel inhibitors which ranges from 9 to 140 μM. The IC_{50} values were deduced from the non linear regression analysis of the log dose response curves.

As shown in Table 1, all inhibitors scaffolds are structurally diverse from each other and from any known MMPIs. With the exception of **5** (and maybe **4**, see paragraph "Active Compounds Binding Modes and Hints for Lead Optimization"), all active compounds possess a carboxylate function as ZBG. Compound **5** which holds a dimethoxybenzene as ZBG retains a certain activity although his IC_{50} (140 μM) is higher than all of the carboxylate-containing inhibitors. Very recently, Novartis researchers reported that a series of carboxylic acids such as the MMP-13 inhibitor **24f**[34] were orally available and equipotent to the most potent hydroxamic acid based inhibitors in *in vivo* models of cartilage protection. Thus, some key physicochemical properties of our five leads were compared to those of **24f**. Table 2 lists pKa, ClogP, ClogD, and TPSA data, which were calculated in silico[35] as useful descriptors to estimate ionization, lipophilicity, and polarity. As shown in Table 2, with the exception of **5**, which seems to be the least drug-like compound, all other inhibitors possess an average value of ClogP ranging from 0.89 to 3.32 and a ClogD and a TPSA very similar to that of **24f**. Thus, with the exception of **5**, all

the others seem to be ideal leads, for which the S1’ substituent could be easily extended and/or modified.

Table 1. Structures, Labels, AD4 Binding Free Energies and IC_{50} of MMP-13 inhibitors identified with VS Experiments.

Chemical Structure	**Life Chemicals Code**	**ΔG_{AD4} (Kcal/mol)**	**IC_{50}[a] (μM)**
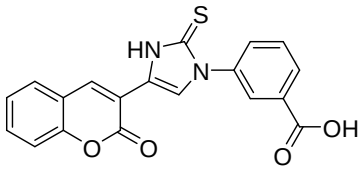 **1**	F0920-6501	-13.33	9
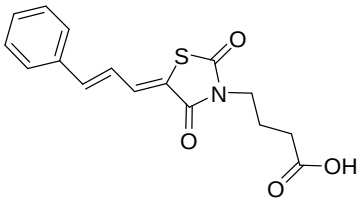 **2**	F1074-0280	-13.12	22
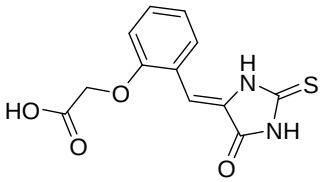 **3**	F1204-0078	-10.96	67
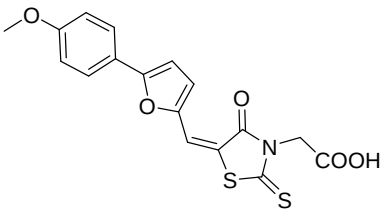 **4**	F1542-0089	-12.11	120
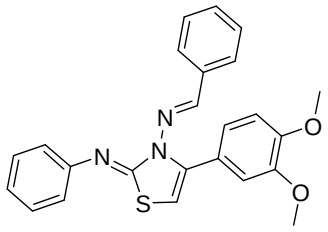 **5**	F0807-0342	-10.5	140

[a] IC_{50} values represent the concentration required to produce 50% enzyme inhibition.

Table 2. Physicochemical Property Predictions of Compounds **1**-**5** and **24f**.

Compd	**pKa** [a]	**ClogP** [b]	**ClogD** [c]	**TPSA (Å)** [d]
1	3.91	3.32	0.11	119.96
2	3.89	2.6	-0.61	99.98
3	3.68	0.89	-2.56	119.75
4	3.62	2.91	-0.42	137.37
5	-	5.55	5.55	71.71
24f[e]	2.55	3.39	-0.13	158.86

[a] pKa predictions refers to the ZBG. [b] Calculated n-octanol/ water partition coefficient. [c] Calculated distribution coefficient at pH=7.4. [d] Topological polar surface area. [e] Orally active carboxylic acid-derived MMP-13 inhibitor used for comparison purpose[34].

2.2 Biological evaluation

The inhibitory activity of the five novel leads was evaluated (Table 3) against a panel of MMP isozymes (MMP-1, -2, -3, 13, -14), some of which are implicated in cartilage degradation. Over the five inhibitors, two (**1** and **4**) are definitely more active on MMP-13 showing appreciably weaker activity on all the other tested enzymes (Table 3). In this respect, both compounds represent appealing leads amenable of structural modification to develop selective MMP-13 inhibitors. Inhibitors **3**, and **5** are equally active on MMP-13 and MMP-14. The two compounds show inhibitory activity also towards MMP-2. In this respect, it is not clear whether this inhibitory profile is beneficial in terms of protecting cartilage degradation. Actually, the role of MMP-2 activity itself in the pathogenesis of OA is unclear. Interestingly, mRNA levels of MMP-2 are increased in OA patients compared to normal controls, suggesting that MMP-2 may play a role in this disease.[36] On the other hand, MMP-2-null mice exhibit a more severe arthritic phenotype than wild type mice in antigen-induced arthritis, suggesting that the total loss of MMP-2 activity is unfavorable.[37] Differently, compound **2** shows a certain preference for MMP-2 (IC_{50} = 2.7 μM) and could be developed as novel antitumor agent.

Table 3. In Vitro[a] Activity (IC_{50} μM Values) of the novel zinc-binders MMP-13 inhibitors towards diverse MMPs

Compd	Life Chemicals Code	MMP-1	MMP-2	MMP-3	MMP-13	MMP-14
1	F0920-6501	400±150	67±3.0	110±15	9±0.5	51±7.0
2	F1074-0280	93±8.0	2.7±0.2	110±26	22±0.6	21±2.0
3	F1204-0078	114±23	61±7.0	77±21	67±10	55±4.0
4	F1542-0089	860±110	350±38	850±200	120±8	310±18
5	F0807-0342	360±46	120±14	230±24	140±10	150±18

[a] Assays were run in triplicate. The final values given here are the mean ± SD of three independent experiments.

2.3 Active Compounds Binding Modes and Hints for Lead Optimization.

Besides the carboxylate function, which, with the exception of **5,** is a conserved feature of all active inhibitors, the five compounds deeply differ in their chemical structures. Indeed, in **1**, the carboxylate moiety is directly attached to a benzene ring, in **2** this portion is linked to a thiazolidindione nucleus by a propyl-linker, while in **3** and **4** a oxymethylene and a methylene bridge, respectively, link the carboxylate group to a benzene and thioxothiazolidinone ring, respectively. Regardless the structural dissimilarities among the aforementioned ligands, all of them are characterized by a small number of rotatable bonds (ranging from 0 to 4). Indeed, the rigidity of **1** allows the proper orientation of the ZBG to chelate the catalytic zinc ion and the P1'group into the S1' pocket (see Figure2).

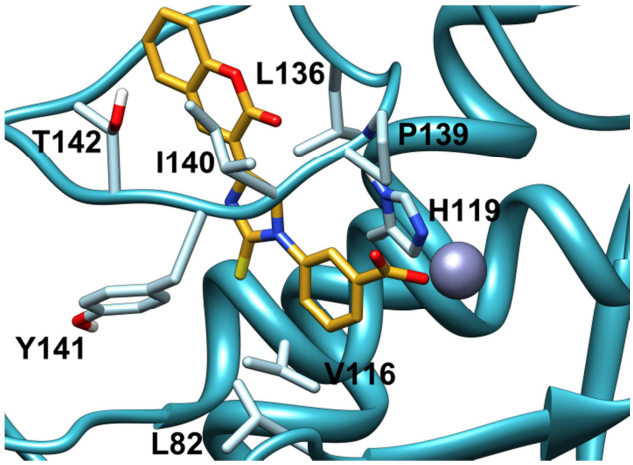

Figure 2. Docked conformations of **1** in the MMP-13 catalytic site. Hydrogens are omitted for the sake of clarity. Ligands carbon atoms are displayed in golden, and key binding site residues as cyan sticks.

The imidazolethione ring is in a suitable position to establish a π -π interaction with H119 side chain. The micromolar IC_{50} for this compound might be due to the non-optimized interaction between the P1' group and the S1' pocket. The selectivity of **1** towards the MMP-13 is surely ascribable to the bulky chromenone nucleus located into the unusually large S1'specificity pocket. In fact, although MMP-13 and -14 possess a S1' specificity loop of the same length, the latter has a narrower shaped S1' pocket, due to the substitution of T245 and T247 in MMP-13 with Q262 and M264 in MMP-14. This hypotheses is confirmed by inhibitor **2** (Fig 3a), which shows the same activity on MMP-13 and MMP-14 possessing a thin olefinic chain ending with a phenyl ring which is unable to fill the roomy S1'pocket. Differently from inhibitor **2**, compound **3** has a small and polar P1' group, and this is the reason for the lower activity and selectivity for MMP-13 with respect to **1** and **2.** However in **3** (Fig 3b)**,** the

thioxoimidazolidinone ring could be substituted with groups featuring shapes and electrostatic propertied able to favorably interact with the peculiar S1' tunnel of MMP-13. Especially for this compound, the extension of the P1' group is certainly a priority step.

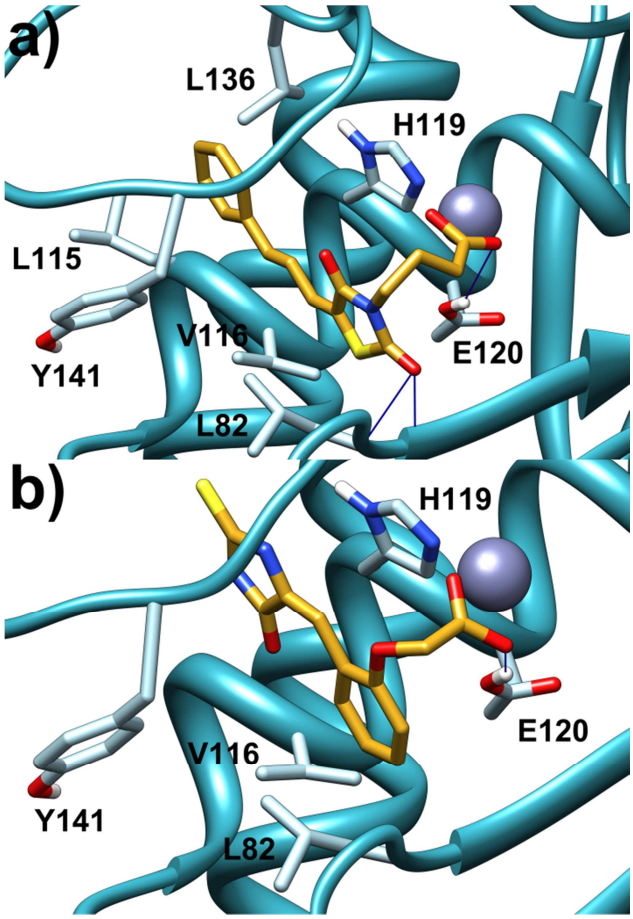

Figure 3. Docked conformations of **2** (a) and **3** (b) in the MMP-13 catalytic site.

As regards compound **4** (Fig 4a), molecular docking unambiguously indicate that the ZBG would be the carboxylate group and not the rhodanine ring via the thiazolidine sulfur atom, as previously found for Anthrax Lethal Factor inhibitors,[38] which have in common with compound **4** both the rhodanine ring and the carboxylate group. However, a search in

the Cambridge Structural Databases shows that, at least in absence of any receptor structure, the carboxylate moiety prevails onto the rhodanine ring in the coordination of metal ions. Thus, prior of any rational optimization, further studies have to be conducted in order to assess the real binding mode of **4** in the MMP-13 active site.

Inhibitor **5** (Fig 4b), is the weakest inhibitor (IC_{50} on MMP-13=140 μM) on the entire panel of MMPs tested, although it is the only one whose P1' group is able to make some contacts with the entrance residues of the S1' pocket like P139, V116, as well as a parallel π-stacking with the H119. The thiazolidine ring makes some lipophilic contacts with the S1' pocket floor residues (L81 and L82), while the N-benzylidene group projects itself towards the beta carbons of the Y141 and the I140.

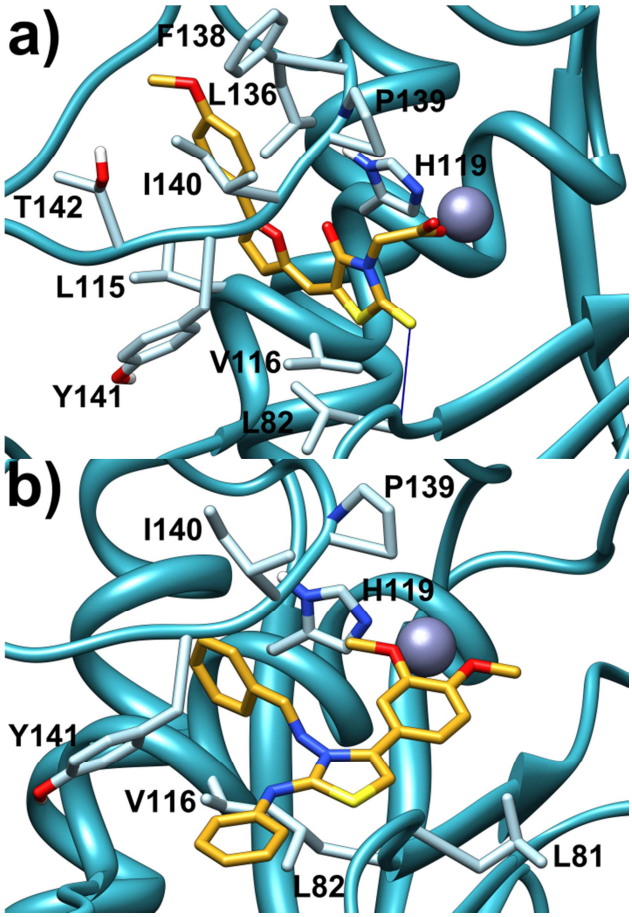

Figure 4. Docked conformations of **4** (a) and **5** (b) in the MMP-13 catalytic site.

In this case, the low activity is ascribable to the presence of a putative weak zinc ion chelator (dimethoxybenzene) and to the fact that it has been tested as a mixture of diastereoisomers. Thus, separation and testing of each single diastereoisomer, together with the substitution of the weak chelator moiety with a stronger one, could be the first step of the lead optimization process of this inhibitor. Subsequent steps could include proper substitutions of both phenyl rings to enhance the interaction with the S1' and S3' pockets.

Thus, generally speaking, none of these compounds has such an extended P1' group to occupy the whole S1' tunnel of the MMP-13,

neither the P1' are well-optimized to interact with the pocket. This is certainly the reason for the inhibitory activities in the range of μM. However, a rationally designed lead optimization project will surely increase the experimental IC_{50}'s. In fact, even if less potent than hydroxamate-based inhibitors, carboxylates could be a valid alternative to this moiety. This weaker zinc-binder could allow to have selective inhibition if present in properly optimized structures. In order to verify the reliability of the proposed binding modes, the de-carboxylated analogue of compound **1** has been synthetized and subjected to binding assay. Intriguingly, the IC50 of this analogue turns out to be 177 μM, proving that our molecules were actually zinc binders as predicted by the docking program. Furthermore, for compound **1**, which show a pretty good selectivity profile, lead optimizations have been carried out.

2.4 Lead Optimization. BOMB Analysis.

At this point, a full substituent scan was indicated for replacement of each aromatic hydrogen in the 2-H-cromen-2-one core of compound **1**. This was carried out with the in-home program BOMB (Biochemical and Organic Model Builder, Prof. William Jorgensen, Yale University, New Haven CT, USA).

A standard protocol for a substituent scan with BOMB is to replace each hydrogen of a core with 10 small groups that have been selected for difference in size, electronic character, and hydrogen-bonding patterns: Cl, CH3, NH2, OH, CH2NH2, CH2-OH, CHO, CN, NHCH3, and OCH3. To begin, the structure of **1** bound to MMP-13 was built with BOMB using the AutoDock best scored pose and the structure of MMP-13 from the 830C PDB file. BOMB was then used to build the 50 complexes corresponding to the replacement of each phenyl hydrogen in the core with the 10 small groups. This revealed that the top-5 scoring analogs are dominated by substitution of either chlorine or oxygen group at the 6- and 8- position in the cromenone ring. Given this information, synthesis of compounds **10**-**13** in Table 4 was carried out. Binding assay of compounds having both positions combinatorially substituted are already ongoing. These latter compounds are supposed to have inhibitor activity in nM range.

Table4. Chemical structure, BOMB score and inhibitor activity of compound 1 and the prepared compounds.

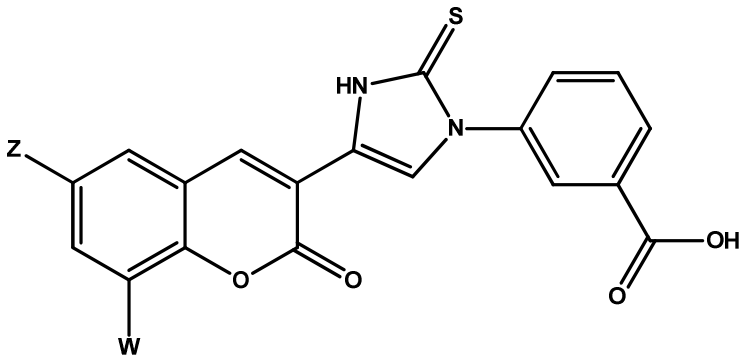

Chemical Structure	W	Z	BOMB Score	IC50(mM)
1	H	H	0	14
10	OH	H	-3.0851	5.5
11	OCH3	H	-2.9863	5.2
12	H	OCH3	-3.0431	3.2
13	H	Cl	-3.4067	2.6

2.5 Ligand-Based VS. ROCS

With the information available for the receptor structure regarding the unique S1'* pocket, we decided to identify small molecule MMP-13 inhibitors through virtual screening using a ligand-based approach called ROCS. As a starting point for the ROCS search, we chose the methylquinazoline-dione allosteric inhibitor co-crystallized in 2OZR pdb structure. The X-ray crystallographic conformation of the ligand was used as a query for ROCS. To identify a novel MMP-13 small molecule inhibitors, ROCS shape-based searches were performed on Maybridge collections. The chemical/or color force field (CFF), Mills Dean, was added to the shape matching procedure during the searches. In other words, after finding the best alignment based on the shape, the program calculates the color force field score (color) to measure chemical complementarities, and to refine shape-based superimpositions based on chemical similarity. A scaled color value is calculated by taking a hit's actual score value and dividing it by the color score of the query molecule against itself. The score used for ranking the hit list in this experiment is combo score that is the sum of the shape Tanimoto coefficient and the scaled color value. Since both shape Tanimoto coefficient and the scaled color are in the range of 0 and 1, the combo score has a value from 0 to 2. Virtual screening hits were selected based on the minimum combo score of 1.2 in the ROCS searches. Thus, 1500 molecules were post-processed with AD4. The binding pocket

was defined using the crystallographic coordinates of the query (residues within 10 Å from the ligand) and only the best ranked 500 molecules were then visual inspected. In order to obtain compounds endowed with an inhibitory potency against MMP-13, all the molecules possessing a central rigid core, with 2 aromatic groups at the two opposite sides of the latter, were retained. Then, for each molecule, the quality of the core has been evaluated on the basis of the interactions established by the query with the MMP-13 enzyme. Particularly, it has been investigated the attitude to form hydrogen bonds with the backbone nitrogens of Thr224, Thr226 and Met232 within the S1'-specificity loop, whereas it has been considered of great importance for the two aromatic regions, their ability to establish π-interactions with His201 and Tyr223 in the S1' pocket, and with Tyr225 and Phe231 within the S1'* cavity. As last criterion of choice, we evaluated the attitude of each molecule to be chemically optimized. After the visual inspection, 40 molecules were finally submitted for testing with the consideration of chemical diversity. Primary binding assays, conducted as mentioned in the previous paragraph, identified four initial hits having inhibitor activity which ranges from 14 to 93 μM (Table 5). The ROCS hits and the query molecule have substantially different chemistry but reasonably high shape similarity. The inhibitory activity of the three most active leads was evaluated (Table 6) against a panel of MMP isozymes (MMP-1, -2, -13, -14), as well as for the leads found through the Receptor-Based VS. Over the three inhibitors, compound **6** is definitely more active

on MMP-13 showing the best selectivity profile among the nine hits found in this work. In this respect, this compound probably represents the most promising lead to develop selective MMP-13 inhibitors with inhibitor activity in nM range. In order to proceed with a lead optimization cycle, a crystal structure of the ligand-protein complex is strictly required

Table 5. Structures, Labels and IC_{50} of MMP-13 inhibitors identified with VS Experiments.

Chemical Structure	**Maybridge Codes**	**IC50[a] (μM)**
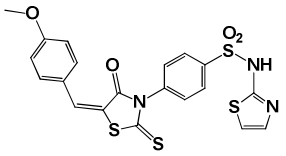 **6**	SO4817	14
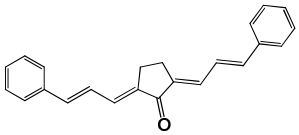 **7**	DP00965	76
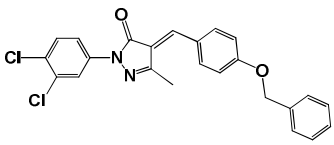 **8**	BTB08190	85
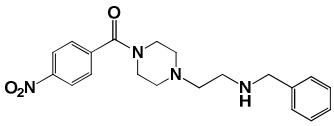 **9**	KM08338	93

[a] IC_{50} values represent the concentration required to produce 50% enzyme inhibition.

Table 6. In Vitro[a] Activity (IC_{50} µM Values) of the novel allosteric MMP-13 inhibitors towards diverse MMPs

Compd	Maybridge Code	MMP-1	MMP-2	MMP-13	MMP-14
6	SO4817	710±110	440±52	14±2.4	290±8.4
7	DP00965	120±9.7	95±8.7	76±5.5	116±8.8
8	BTB08190	300±35	150±16	85±7.1	200±8.8

[a] Assays were run in triplicate. The final values given here are the mean ± SD of three independent experiments.

Experimental Section

Databases Preparation

For the in silico screening, the Life Chemicals database[39] and the Maybridge database were used. These libraries are a collection of small compounds carefully selected to provide the broadest pharmacophore coverage for a total of 6000 and 70000 non-redundant molecules, respectively. The databases were uploaded on ZINC server[40] as 1D smiles strings and processed with the ZINC protocol. This protocol filters-out molecules with molecular weight greater than 700, calculated LogP greater than 6 and less than −4, number of hydrogen-bond donors, hydrogen-bond acceptors, and rotatable bonds greater than 6, 11, and 15 respectively. It also removes all molecules containing “exotic” atoms (i.e. different from H, C, N, O, F, S, P, Cl, Br, or I). Moreover it allows the creation of all stereoisomers, tautomers and correctly protonated forms of the molecules between pH 5 and 9.5. The protocol outcome from the server was a file containing 7769 and 79229 compounds, respectively.

Selection of the MMP-13 X-ray Structure for VS experiment and Protein Preparation

Eighteen X-ray structures of MMP-13 have been released in the Protein Data Bank (PDB). A superposition of all X-ray structures on the alpha carbon atoms, using 830C as reference structure, shows that the

protein folding and the catalytic loops shape are highly superimposable and that in the catalytic site, the large majority of the residues are all preserved in the side chain conformations. Thus, only the enzyme structure 830C, which has the lower resolution (1.60 Å), was selected for our VS experiment. From this structure, all water molecules, ions and the inhibitor were removed from the binding site. All hydrogen atoms were added to the protein structure using ADT,[41] and to the catalytic Zn ion present in the active site a +2 charge was assigned.

Receptor-Based Virtual Screening Calculations

Docking calculations were performed with version 4.0 of the AutoDock software package as implemented through the graphic user interface AutoDockTools (ADT 1.4.6). All compounds of the Life Chemical diversity set together with the 830C structure of MMP-13 were converted to AutoDock format files (.pdbqt) using ADT. The docking area was defined by a box, centered on the catalytic zinc. Grids (dimension of 60 Å × 65 Å × 60 Å) were then generated for 13 ligand atom types (sufficient to describe all atoms in the selected database) with the help of AutoGrid4 using a grid spacing of 0.375 Å. For each ligand of the Life Chemical diversity set, 100 separate docking calculations were performed. Each docking calculation consisted of 1 × 107 energy evaluations using the Lamarckian genetic algorithm local search (GALS) method. A low-

frequency local search in accordance with the method of Solis and Wets was applied to docking trials to ensure that the final solution represents a local minimum. Each docking run was performed with a population size of 150, and 300 rounds of Solis and Wets local search were applied, with a probability of 0.06. A mutation rate of 0.02 and a crossover rate of 0.8 were used to generate new docking trials for subsequent generations. The docking results from each of the 100 calculations were clustered on the basis of root-mean square deviation (rmsd 2 Å) between the Cartesian coordinates of the ligand atoms and were ranked on the basis of the free energy of binding. The top-ranked compounds were visually inspected for good chemical geometry. Finally, as a last criterion of selection, we introduced the visual inspection of the putative best ranking ligand/receptor complexes. In this regard, we decided to discard all the molecules for which AD4 did not predict coordination of the catalytic zinc in order to obtain compounds of a certain potency. Another selection criterion resided in the occupancy of the S1' pocket, in the attempt to obtain a selectivity of action towards the MMP-13. Pictures of the modelled ligand/enzyme complexes together with graphic manipulations were rendered with UCSF Chimera package from the Resource for Biocomputing, Visualization, and Informatics at the University of California, San Francisco.[42]

Ligand-Based OMEGA/ROCS Calculations

ROCS uses atom centered Gaussian functions parametrized to provide close approximations to hard sphere volumes. In ROCS, shape-similarity is evaluated by maximizing the volume overlap between the reference active compound and a single conformation of a query molecule using the Tanimoto coefficient. In version 2.3.1, used in this study, a “color force field” represents physicochemical properties in addition to the shape component. The conformational search of the different query compounds (up to 100 conformers per compound) has been carried out prior to all the calculations using OMEGA, version 2.1.33

BOMB Analysis

BOMB creates analogs by adding substituents to a core that has been placed in a binding site.3a A thorough conformational search is performed for each analog, and the position, orientation, and dihedral angles for the analog are optimized using the OPLS-AA force field for the protein and OPLS/CM1A for the analog.8 The protein is rigid except for optimization of the terminal dihedral angles for side chains with hydrogen-bonding groups (e.g., the OH of tyrosine and the carboxylate group of aspartate). The resultant conformer for each analog with the lowest energy is then

evaluated with a docking-like scoring function. The current scoring function has been trained to reproduce experimental activity data for 339 complexes of HIV-RT, COX-2, FK506 binding protein (FKBP), and p38 kinase. The scoring function only contains five descriptors that were obtained by linear regression: the octanol/water partition coefficient for the analog as computed by QikProp (QPlogPo/w), the amount of hydrophobic surface area for the protein that is buried upon complex formation (¢FOSAP), the number of potential hydrogen-bond donating hydrogens in the analog (HBDNL), the number of nonconjugated amides in the analog, and the number of "bad" protein-analog contacts in the complex (NBAD). The latter represent structural mismatches between two atoms within 4 Å, typically between a potential hydrogen-bonding oxygen or nitrogen and a saturated carbon atom or between a potential hydrogen-bond accepting O or N and another such atom or an aryl carbon atom. Interestingly, (a) the most significant descriptor is QPlogPo/w, which alone yields a fit with an r2 of 0.47, and (b) inclusion of energetic results from full conjugate-gradient optimizations of the complexes created by BOMB was found to have little impact on the accuracy of the scoring. Although the BOMB scoring is still under development, the current version provides a useful evaluation of potential activity.

Chemistry

The purity of the five hits that were essential to the conclusions drawn in the text were determined by HPLC on a Merck Hitachi D-7000 liquid chromatograph equipped with a Discovery C18 column (250 mm x 4.6 mm, 5 μm particle size) and a UV/vis detector setting at λ=250 nm.

Biology. Materials and Methods.

Recombinant human MMP-14 catalytic domain was a kind gift of Prof. Gillian Murphy (Department of Oncology, University of Cambridge, UK). Pro-MMP-1, pro-MMP-2, pro-MMP-3, and pro-MMP-13 were purchased from Calbiochem. APMA was from Sigma-Aldrich. All compounds were subjected to combustion analysis prior to be tested for their inhibitory activity, to verify their consistence with a purity of at least 95%. ARP100 was synthesized at Department of Pharmaceutical Sciences (Pisa, Italy) according to the previously described procedure.[32] All other chemicals were of reagent grade.

Enzyme activation.

Proenzymes were activated immediately prior to use with p-aminophenylmercuric acetate (APMA 2 mM for 1 h at 37 °C for MMP-2, APMA 2 mM for 2 h at 37 °C for MMP-1, 1 mM for 30 min at 37 °C for MMP-13). Pro-MMP-3 was activated with trypsin 5 µg/mL for 30 min at 37 °C followed by soybean trypsin inhibitor 62 µg/mL.

Enzyme inhibition assays.

For assay measurements, the purchased compound stock solutions (10 mM in DMSO) were further diluted for each MMP in the fluorimetric assay buffer (FAB: Tris 50 mM, pH = 7.5, NaCl 150 mM, CaCl2 10 mM, Brij 35 0.05% and DMSO 1%). Activated enzyme (final concentration 0.56 nM for MMP-2, 0.3 nM for MMP-13, 5 nM for MMP-3, 1 nM for MMP-14cd, and 2.0 nM for MMP-1) and inhibitor solutions were incubated in the assay buffer for 4 h at 25 °C. After the addition of 200 µM solution of the fluorogenic substrate Mca-Arg-Pro-Lys-Pro-Val-Glu-Nva-Trp-Arg-Lys(Dnp)-NH2 (Sigma) for MMP-3 and Mca-Lys-Pro-Leu-Gly-Leu-Dap(Dnp)-Ala-Arg-NH2 (Bachem) for all the other enzymes in DMSO (final concentration 2 µM), the hydrolysis was monitored every 15 sec for 15 min recording the increase in fluorescence (λex = 325 nm, λem = 395 nm) using a Molecular Devices SpectraMax Gemini XS plate reader. The

assays were performed in triplicate in a total volume of 200 μL per well in 96-well microtitre plates (Corning, black, NBS). The MMP inhibition activity was expressed in relative fluorescent units (RFU). Percent of inhibition was calculated from control reactions without the inhibitor. The inhibitory effect of the tested compounds was routinely estimated at a concentration of 100 μM towards MMP-13. Those derivatives found to be active were tested at additional concentrations and IC50 was determined using at least five concentrations of the inhibitor causing an inhibition between 10% and 90%, using the formula: $Vi/Vo = 1/(1 + [I]/ IC50)$, where Vi is the initial velocity of substrate cleavage in the presence of the inhibitor at concentration [I] and Vo is the initial velocity in the absence of the inhibitor. Results were analyzed using SoftMax Pro software[43] and Origin 6.0 software.

Conclusions

This paper reports the identification of structurally non-classic MMP-13 inhibitors by means of two different in silico screening methods. Experimental evaluation of a restricted number of candidates (60), which were selected by visual inspection of the poses predicted for the best scoring compounds, led to the identification of five novel zinc-chelating non-hydroxamate inhibitors, and four allosteric inhibitors, structurally distinct from those already reported. Eight of these compounds may provide scaffolds upon which to develop compounds with more desirable properties, such as selectivity of action and oral availability. Moreover, their discovery supports the use of virtual screening as a successful method for the discovery of novel MMPIs with unexpected structures.

REFERENCES

(1) Mort, J. S.; Billington, C. J. Articular cartilage and changes in arthritis: matrix degradation. *Arthritis Res*. **2001**, *3*, 337-341.

(2) (a) Billinghurst, R. C.; Dahlberg, L.; Ionescu, M.; Reiner, A.; Bourne, R.; Rorabeck, C.; et al. Enhanced cleavage of type II collagen by collagenases in osteoarthritic articular cartilage. *J. Clin. Invest.* **1997**, *99*, 1534-1545. (b) Billinghurst, R. C.; O'Brien, K.; Poole, A. R.; McIlwraith, W. Inhibition of articular cartilage degradation in culture by a novel nonpeptidic matrix metalloproteinase inhibitor. *Ann. N. Y. Acad. Sci.* **1999**, *878*, 594-597. (c) Jüngel, A.; Ospelt, C.; Lesch, M.; Thiel, M.; Sunyer, T.; Schorr, O.; Michel, B. A.; Gay R. E.; Kolling, C.; Flory, C.; Gay, S.; Neidhart, M. Effect of the oral application of a highly selective MMP-13 inhibitor in three different animal models of rheumatoid arthritis. *Ann. Rheum. Dis.* **2009**.

(3) (a)Aranapakam, V.; Davis J.M.; Grosu, G. T.; Baker, J.; Ellingboe, J.; Zask, A.; et al. Synthesis and structure-activity relationship of N-substituted 4-arylsulfonylpiperidine-4-hydroxamic acids as novel, orally active matrix metalloproteinase inhibitors for the treatment of osteoarthritis. *J. Med. Chem.* **2003**, *46*, 2376-2396. (b) Sabatini, M.; Lesur, C.; Thomas, M.; Chomel, A.; Anract, P.; deNanteuil, G.; et al. Effect of inhibition of matrix metalloproteinases on cartilage loss in vitro and in a guinea pig model of osteoarthritis. *Arthritis Rheum.* **2005**, 52, 171-180. (c)

Baragi, V. M.; Becher, G.; Bendele, A. M.; Biesinger, R.; Bluhm, H.; Boer, J.; Deng, H.; Dodd, R.; Essers, M.; Feuerstein, T.; Gallagher, B. M. Jr., Gege, C.; Hochgürtel, M.; Hofmann, M.; Jaworski, A.; Jin, L.; Kiely, A.; Korniski, B.; Kroth, H.; Nix, D.; Nolte, B.; Piecha, D.; Powers, T. S.; Richter, F.; Schneider, M.; Steeneck, C.; Sucholeiki, I.; Taveras, A.; Timmermann, A.; Van Veldhuizen, J.; Weik, J.; Wu, X.; Xia, B. A new class of potent matrix metalloproteinase 13 inhibitors for potential treatment of osteoarthritis: Evidence of histologic and clinical efficacy without musculoskeletal toxicity in rat models. *Arthritis Rheum.* **2009,** *60*, 2008-2018.

(4) Renkiewicz, R.; Qiu, L.; Lesch, C.; Sun, X.; Devalaraja, R.; Cody, T.; et al. Broad-spectrum matrix metalloproteinase inhibitor marimastat–induced musculoskeletal side effects in rats. *Arthritis Rheum*. **2003**, *48*, 1742-1749.

(5) Wu, H.; Du, J.; Zheng, Q. Expression of MMP-1 in cartilage and synovium of experimentally induced rabbit ACLT traumatic osteoarthritis: immunohistochemical study. *Rheumatol. Int.* **2008**, *29*, 31-36.

(6) Li, J. J.; Nahra, J.; Johnson, A. R.; Bunker, A.; O0Brien,P.;Yue,W. S.;Ortwine,D. F.;Man, C. F.;Baragi, V.; Kilgore, K.; Dyer, R. D.; Han, H. K. Quinazolinones and pyrido-[3,4-d]pyrimidin-4-

ones as orally active and specific matrix metalloproteinase-13 inhibitors for the treatment of osteoarthritis. *J. Med. Chem.* **2008**, *51*, 835–841.

(7) Nuti, E.; Casalini, F.; Avramova, S. I.; Santamaria, S.; Cercignani, G.; Marinelli, L.; La Pietra, V.; Novellino, E.; Orlandini, E.; Nencetti S.; Tuccinardi, T.; Martinelli, A.; Lim, N. H.; Visse, R.; Nagase, H.; Rossello, A. N-O-isopropyl sulfonamido-based hydroxamates: design, synthesis and biological evaluation of selective matrix metalloproteinase-13 inhibitors as potential therapeutic agents for osteoarthritis. *J. Med. Chem.* **2009**, *52*, 4757-4773.

(8) Flipo M, Charton J, Hocine A, Dassonneville S, Deprez B, Deprez-Poulain R. Hydroxamates: Relationships between Structure and Plasma Stability. *J. Med. Chem.* **2009**, *in press*.

(9) Nuti, E.; Panelli, L.; Casalini, F.; Avramova, S. I.; Orlandini, E.; Santamaria, S.; Nencetti, S.; Tuccinardi, T.; Martinelli, A.; Cercignani, G.; D'Amelio, N.; Maiocchi, A.; Uggeri, F.; Rossello, A. Design, Synthesis, Biological Evaluation, and NMR Studies of a New Series of Arylsulfones As Selective and Potent Matrix Metalloproteinase-12 Inhibitors. *J. Med. Chem.* **2009**, 52, 6347–6361.

(10) Hidalgo S., Eckhardt S.G., Development of Matrix Metalloproteinase Inhibitors in Cancer Therapy, 2001, *Journal of the National Cancer Institute, 93, 178-193*.

(11) Gomez DE, Alonso DF, Yoshiji H, Thorgeirsson UP. Tissue inhibitors of metalloproteinases: structure, regulation and biological functions. *Eur J Cell Biol*, **1997**, *74, 111–22.*

(12) Murphy G, Stanton H, Cowell S, Butler G, Knauper V, Atkinson S, et al. Mechanism for pro matrix metalloproteinase activation. *APMIS, **1999,** 107, 38–44*

(13) Roswell, S., Hatwin, P., Minshull, C. A., Jepson, H., Brockbank, S. M. V., Barratt, D. G., Slater, A. M., McPheat, W. L., Waterson, D., Henney, A. M., and Pauptit, R. A., *J. Mol. Biol. **2002**,319, 173–181*

(14) S1' nomenclature Schechter, I., and Berger, A., *Biochem. Biophys. Res. Commun., **1967**, 27, 157–162*

(15) Johnson AR.; Pavlovsky AG.; Ortwine DF.; Prior F.; Man CF.; Bornemeier DA.; Banotai CA.; Mueller WT.; McConnell P.; Yan C.; Baragi V.; Lesch C.; Roark WH.; Wilson M.; Datta K.; Guzman R.; Han HK.; Dyer RD.; *The Journal of Biological Chemistry, **2007**, 282, 27781–27791*

(16) Venhorst, J.; Nùñez, S.; Terpstra, J. W.; Kruse, C. G. *J. Med. Chem.* **2008**, 51, 3222–3229

(17) Guner, O. F.; Hughes, D. W.; Dumont, L. M. An integrated approach to three-dimensional information management with MACCS-3D. *J. Chem. Inf. Comput. Sci.* ***1991****, 31, 408–414*

(18) Good, A. C.; Hermsmeier, M. A.; Hindle, S. A. Measuring CAMD technique performance: A virtual screening case study in the design of validation experiments. *J. Comput.-Aided Mol. Des.* ***2004****, 18, 529–536*

(19) Schneider, G.; Neidhart, W.; Giller, T.; Schmid, G. Scaffold-hopping by topological pharmacophore search: A contribution to virtual screening. *Angew. Chem., Int. Ed. Engl.* ***1999****, 38, 2894–2896*

(20) Kirchmair, J.; Ristic, S.; Eder, K.; Markt, P.; Wolber, G.; Laggner, C.; Langer, T. Fast and efficient in silico 3D screening: Toward maximum computational efficiency of pharmacophore-based and shape-based approaches. *J. Chem. Inf. Model.* ***2007****, 47, 2182– 2196*

(21) a)Putta, S.; Eksterowicz, J.; Lemmen, C.; Stanton, R. A novel subshape molecular descriptor. J. Chem. Inf. Comput. Sci. **2003**, 43, 1623– 1635.; b) Haigh, J. A.; Pickup, B. T.; Grant, J. A.; Nicholls, A. Small molecule shape-fingerprints. *J. Chem. Inf. Model.* ***2005****, 45, 673–684*

(22) Kroemer, R. T. Structure-based drug design: Docking and scoring. *Curr. Protein Pept. Sci.* ***2007****, 8, 312–328*

(23) a) Dror, O.; Shulman-Peleg, A.; Nussinov, R.; Wolfson, H. J. Predicting molecular interactions in silico: A guide to pharmacophore identification and its applications to drug design. *Curr. Med. Chem.* ***2004***, *11, 71–90*

(24) Grant, J.A., Gallardo, M.A., Pickup, B., *J. Comp. Chem.*, ***1996***, *17, 1653.*

(25) Rush, T.S., Grant, J.A., Mosyak, L., Nicholls, A., *J. Med. Chem.*, ***2005***, *48, 1489.*

(26) Hawkins, P.C.D., Skillman, A.G., Nicholls, A., *J. Med. Chem.*, ***2007***, *50, 74.*

(27) Venhorst, J., Nunez, S., Terpstra, J.W., Kruse, C.G., *J. Med. Chem.*, ***2008***, *51, 3222.*

(28) Sheridan, R.P., McGaughey, G.B., Cornell, W.D., *J. Comput. Aided Mol. Des.*, ***2008***, *22, 257.*

(29) Sutherland, J.J., Nandigam, R.K., Erickson, J.A., Vieth, M. *J. Chem. Inf. Model*, ***2007***, *49, 1715.*

(30) Huey, R.; Morris, G. M.; Olson, A. J.; Goodsell, D. S. A semi-empirical free energy force field with charge-based desolvation. *J. Comput. Chem.* ***2007***, *28, 1145–1152.*

(31) (a)Sandro Cosconati, Luciana Marinelli, Roberta Trotta, Ada Virno, Luciano Mayol, Ettore Novellino, Arthur J. Olson and Antonio

Randazzo. Tandem Application of Virtual Screening and NMR Experiments in the Discovery of Brand New DNA Quadruplex Groove Binders. *J. Am. Chem. Soc.*, i*n press*. (b) Cosconati, S.; Hong J. A.; Novellino, E.; Carroll K. S.; Goodsell D. S.; Olson A. J. Structure-Based Virtual Screening and Biological Evaluation of Mycobacterium tuberculosis Adenosine 5′-Phosphosulfate Reductase Inhibitors. *J. Med. Chem.* **2008,** *51*, 6627-6630. (c) Cosconati, S.; Marinelli, L.; La Motta, C.; Sartini, S.; Da Settimo, F.; Olson, A. J.; Novellino, E. Pursuing aldose reductase inhibitors through in situ cross-docking and similarity-based virtual screening. *J Med Chem.* **2009**, *52*, 5578-5581.

(32) Rossello, A.; Nuti, E.; Orlandini, E.; Carelli, P.; Rapposelli, S.; Macchia, M.; Minutolo, F.; Carbonaro, L.; Albini, A.; Benelli, R.; Cercignani, G.; Murphy, G.; Balsamo, A. New N-arylsulfonyl-N-alkoxyaminoacetohydroxamic acids as selective inhibitors of gelatinase A (MMP-2). *Bioorg. Med. Chem.* **2004**, *12*, 2441-2450.

(33) (a)McGovern, S. L.; Caselli, E.; Grigorieff, N.; Shoichet, B. K. A common mechanism underlying promiscuous Inhibitors from virtual and high-throughput screening. *J. Med. Chem.* **2002**, *45*, 1712–1722. (b) McGovern, S. L.; Helfand, B. T.; Feng, B.; Shoichet, B. K. A specific mechanism of non-specific inhibition. *J. Med. Chem.* **2003**, *46*, 4265–4272.

(34) Monovich, L. G.; Tommasi R. A.; Fujimoto, R. A.; Blancuzzi, V.; Clark, K.; Cornell, W.D.; Doti, R.; Doughty, J.; Fang, J.;

Farley, D.; Fitt, J.; Ganu, V.; Goldberg, R.; Goldstein, R.; Lavoie, S.; Kulathila R.; Macchia, W.; Parker, D. T.; Melton, R.; O'Byrne, E.; Pastor, G.; Pellas, T.; Quadros, E.; Reel, N.; Roland, D. M.; Sakane, Y.; Singh, H.; Skiles, J.; Somers, J.; Toscano, K; Wigg, A.; Zhou, S.; Zhu, L.; Shieh, W. C.; Xue, S.; McQuire, L. W. Discovery of potent, selective, and orally active carboxylic acid based inhibitors of matrix metalloproteinase-13. *J. Med. Chem.* **2009**, *52*, 3523-3538.

(35) The pKa, CLogP, CLogD calculations were performed with the chemsilico server on the web site: http: //chemsilico.com. The TPSA calculation was performed with Marvin Sketch and Calculator Plugins on the web-Site: http://www.chemaxon.com/demosite/marvin/index.html.

(36) Kevorkian, L.; Young, D. A.; Darrah, C.; Donell, S. T.; Shepstone, L.; Porter, S.; Brockbank, S. M.; Edwards, D. R.; Parker, A. E.; Clark, I. M. Expression profiling of metalloproteinases and their inhibitors in cartilage. *Arthritis Rheum.* **2004**, *50*, 131–141.

(37) Itoh, T.; Matsuda, H.; Tanioka, M.; Kuwabara, K.; Itohara, S.; Suzuki, R. The role of matrix metealloproteinase-2 and matrix metalloproteinase-9 in antibody induced arthritis. *J. Immunol.* **2002**, *169*, 2643–2647.

(38) Johnson, S.L., Jung, D., Forino, M., Chen, Y., Satterthwait, A., Rozanov, D.V., Strongin, A.Y., Pellecchia M. Anthrax lethal factor

protease inhibitors: synthesis, SAR, and structure-based 3D QSAR studies. *J. Med. Chem.* **2006**, 49, 27-30.

(39) www.lifechemicals.com

(40) http://zinc.docking.org

(41) Huey, R.; Morris, G. M.; Olson, A. J.; Goodsell, D. S. A semiempirical free energy force field with charge-based desolvation. *J. Comput. Chem.* **2007**, *28*, 1145-1152.

(42) UCSF Chimera--a visualization system for exploratory research and analysis. Pettersen EF, Goddard TD, Huang CC, Couch GS, Greenblatt DM, Meng EC, Ferrin TE. *J Comput Chem.* **2004**, *25*, 1605-1612.

(43) SoftMax Pro 4.7.1 by Molecular Devices.